Journal of Fluorine Chemistry 129 (2008) 613–620

Contents lists available at ScienceDirect

Journal of Fluorine Chemistry

journal homepage: www.elsevier.com/locate/fluor

# Novel methacrylate copolymers with fluorine containing: Synthesis, characterization, reactivity ratios, thermal properties and biological activity

Ibrahim Erol *

*Department of Chemistry, Faculty of Arts and Science, University of Afyon Kocatepe, Afyon, Turkey*

ARTICLE INFO

*Article history:*
Received 20 January 2008
Received in revised form 1 May 2008
Accepted 1 May 2008
Available online 8 May 2008

*Keywords:*
Methacrylate
Fluorine
Monomer reactivity ratios
Biological activity
Thermal stability

ABSTRACT

New methacrylate based monomers 2-(4-benzoylphenoxy)-2-oxoethyl-2-methylacrylate (BOEMA), 2-(4-acetylphenoxy)-2-oxoethyl-2-methylacrylate (AOEMA), and 2-[(4-fluorophenyl)amino]-2-oxoethyl-2-methylacrylate (FPAMA), were synthesized first time. The free-radical-initiated copolymerization of AOEMA and BOEMA with FPAMA were carried out in 1,4-dioxane solution at 65 °C using 2,2′-azobisisobutyronitrile (AIBN) as an initiator with different monomer-to-monomer ratios in the feed. The monomers and copolymers were characterized by FTIR, $^{1}$H NMR and $^{13}$C NMR spectral studies. The copolymer compositions were evaluated by nitrogen content in polymers. The reactivity ratios of the monomers were determined by the application of Fineman–Ross and Kelen–Tudos methods. The analysis of reactivity ratios revealed that BOEMA and AOEMA are less reactive than FPAMA, and copolymers formed are statistically in nature. The molecular weights ($\overline{M}_w$ and $\overline{M}_n$) and polydispersity index of the polymers were determined using gel permeation chromatography. Thermogravimetric analysis of the polymers reveals that the thermal stability of the copolymers increases with an increase in the mole fraction of FPAMA in the copolymers. Glass transition temperatures of the copolymers were found to decrease with an increase in the mole fraction of FPAMA in the copolymers. The prepared homo and copolymers were tested for their antimicrobial activity against bacteria, fungi and yeast.



## 1. Introduction

Fluorine-containing polymers are particularly attractive and useful compounds because of their unique properties including high thermal, chemical, aging and weather resistance, low dielectric constants, refractive index, surface energy and flammability. In addition to these their excellent inertness to solvents, hydrocarbons, acids, alkalis and moisture adsorption as well as interesting oil and water repellency due to the low polarizability and the strong electronegativity of the fluorine atom can be considered as the advantages [1–7]. Consequently, fluorine-containing polymers have widespread applications in modern technologies ranging from building, automotive and aerospace industries to optics and microelectronics [8,9]. So far, the investigations on fluorine-containing polymers emulsion, especially on fluorine-containing methacrylate emulsion have attracted many researchers. There are various approaches for preparing fluorine-containing acrylate emulsion, such as producing block, graft or random fluorine-containing acrylate copolymers [10–13], blending fluorine-containing acrylate polymers and fluorine-free acrylate polymers [14–16] and synthesizing core–shell fluorine-containing polyacrylate emulsion with fluorine-free acrylate and fluorine-containing acrylate monomers [17–22]. Reactivity ratios are among the most important parameters for composition equation of copolymers, which can offer information such as relative reactivity of monomer pairs and estimate the copolymer composition. Knowledge of the copolymer composition is an important step in the evaluation of its utility. Copolymer composition and its distribution depend on the reactivity ratios. The most common mathematical model of copolymerization is based on finding the relationship between the composition of copolymers and the composition of the monomer feed in which the monomer reactivity ratios are the parameters to be determined. The calculation of the monomer reactivity ratios requires the mathematical treatment of experimental data on the compositions of copolymers and monomer feed mixtures. Monomer reactivity ratios are generally determined at low conversion. In the classic terminal model of copolymerization, it has been suggested that, for a given pair of monomers, the instantaneous copolymer composition is only a function of instantaneous feed. Among several methods available to determine monomer reactivity ratio values, the Finemann–Ross and Kelen–Tudos methods are appropriate for the determination of monomer reactivity ratios

* Tel.: +90 272 2281311/227; fax: +90 272 2281235.
*E-mail addresses:* ierol@aku.edu.tr, iberol@hotmail.com.

0022-1139/$ – see front matter © 2008 Elsevier B.V. All rights reserved.
doi:10.1016/j.jfluchem.2008.05.002

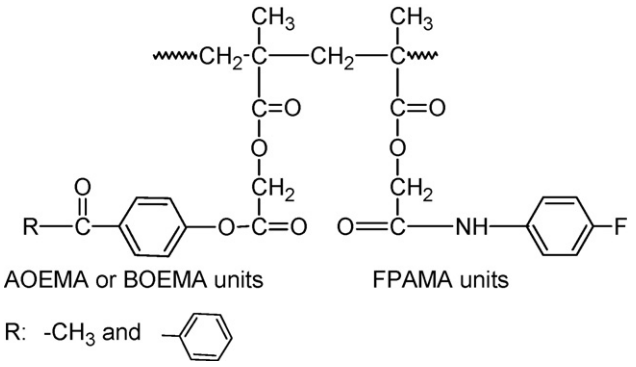


**Scheme 1.**

at low conversions. Thermogravimetric analysis (TGA) has been widely used to investigate the decomposition characteristics of many materials. Some methods have already been established to evaluate the kinetic parameters from thermogravimetric data [23,24].

AOEMA and BOEMA are new methacrylate monomers having pendant ketone side chain. FPAMA is also new methacrylate monomer having pendant amide and fluorine group. In previous studies, the synthesis, characterization and copolymerization behavior of similarly monomers and their polymers have been described [25,26]. However, no studies on reactivity ratios in the copolymerizations of AOEMA and BOEMA with FPAMA appear in the literature. The present article investigates the synthesis, structural, and thermal characterization of copolymers of FPAMA with AOEMA and BOEMA as well as the determination of reactivity ratios in the copolymerization. The biological activities and activation energies of the copolymers were also obtained. For this purpose reactivity ratios $r_1$ and $r_2$ for the classical copolymerization model were determined using the linearization methods of Fineman–Ross (FR method) and Kelen–Tudos (KT method) [27,28].

## 2. Results and discussion

### 2.1. Structural characterization of the copolymers

The constituent monomeric units of the copolymer are as follows (Scheme 1).

The FTIR spectrum of poly(AOEMA-*co*-FPAMA) is shown in Fig. 1. The absorption peak at 3080 $cm^{-1}$ is due to aromatic C–H stretching. The peaks at 2950 and 2860 $cm^{-1}$ are due to C–H stretching of methyl and methylene groups. The strong absorptions at 1784, 1740 and 1683 $cm^{-1}$ in the IR spectra of poly(AOEMA-*co*-FPAMA)s are due to the carbonyl stretching of ester carbonyl (in AOEMA unit), methacryl carbonyl for both monomeric units and amide carbonyl stretching for FPAMA units, respectively. The band at 3230 $cm^{-1}$ (–NH in the PAMA unit) is the most characteristic for the copolymer. The aromatic C=C stretching appears at about 1590 and 1465 $cm^{-1}$. The medium absorption peaks at 1180 $cm^{-1}$ is attributed to the C–O stretch of the ester group. Peaks at 750–780 and 1030–1100 $cm^{-1}$ may be assigned to the aromatic C–H out-of-plane bending and in-of-plane bending (for *p*-disubstitue benzene ring for both monomeric units), respectively, and those at 1450 $cm^{-1}$ may be assigned to $CH_3$ bending vibrations.

The $^1H$ NMR and $^{13}C$ NMR spectrums of poly(AOEMA-*co*-FPAMA) are shown in Fig. 2a and b, respectively. The $^1H$ NMR spectrum of poly(AOEMA-*co*-FPAMA) is consistent with its chemical structure. Multiplet resonance absorptions at 6.8–8.0 ppm are due to the aromatic protons of AOEMA and FPAMA. The NH protons of FPAMA resonance appears at 8.5 ppm. The signals at 4.2–4.6 ppm are due to $-OCH_2$ protons of two monomeric unit. The methoxy protons of AOEMA resonance appears at 3.3 ppm. The backbone methylene protons of the two comonomer units are observed between 1.7 and 1.9 ppm. The α-methyl protons of monomer units are observed at 0.9–1.1 ppm. The chemical shift assignments were made from the off-resonance decoupled spectra of the copolymers. In the proton decoupled $^{13}C$ NMR spectrum of copoly(AOEMA-*co*-FPAMA), the resonance

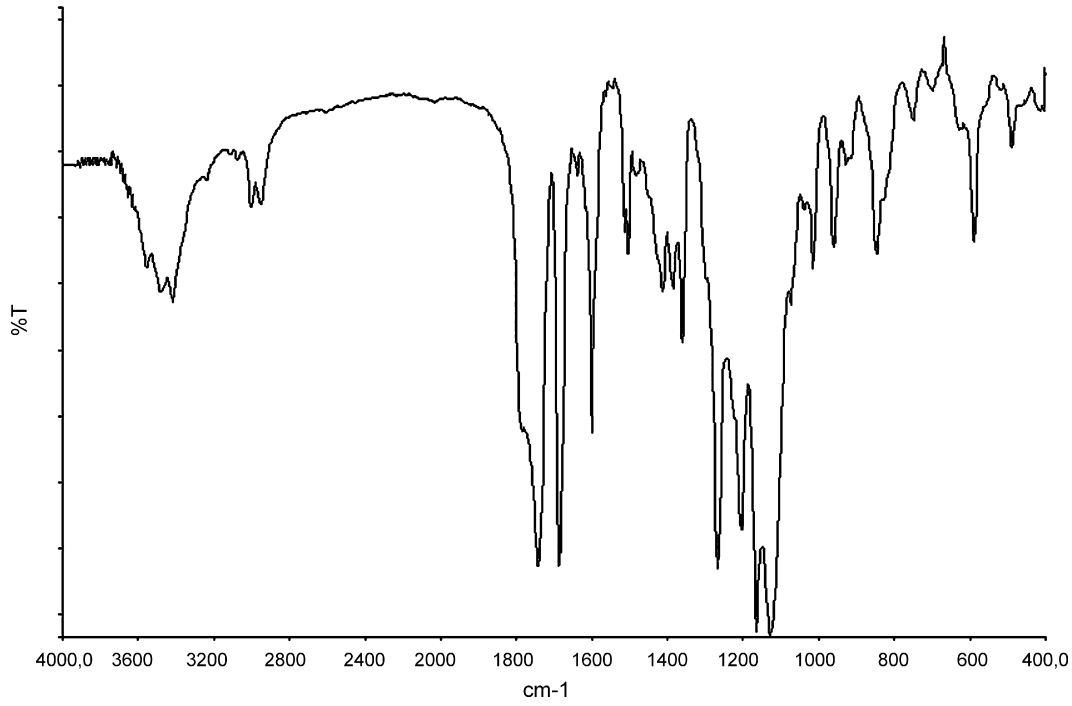


**Fig. 1.** FTIR spectrum of poly(AOEMA-*co*-FPAMA); $m_1$:$m_2$ [45:55].

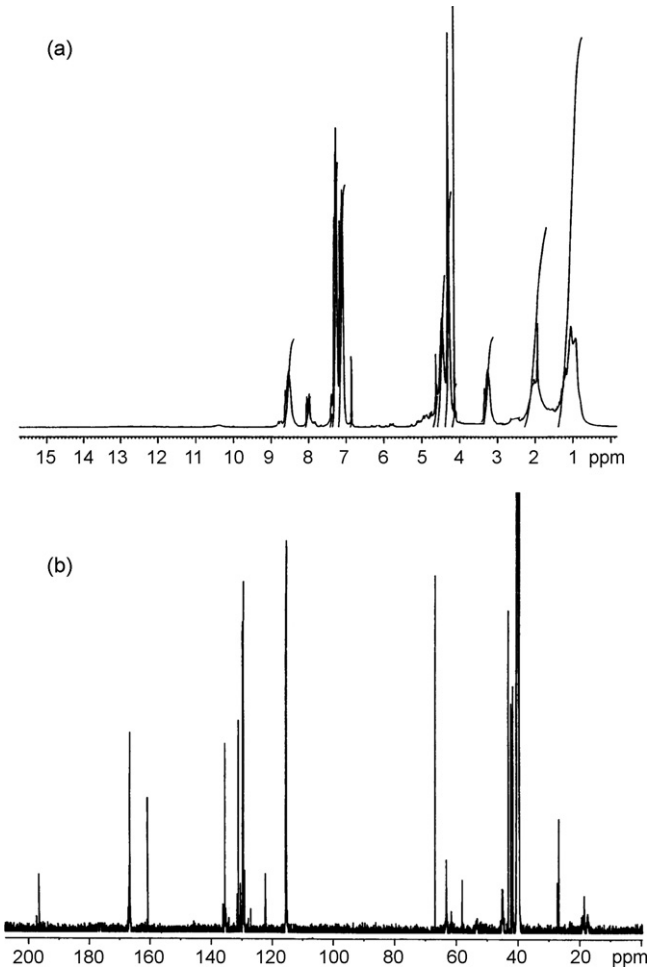


**Fig. 2.** $^{1}$H NMR and $^{13}$C NMR spectrum of poly(AOEMA-*co*-FPAMA); $m_1$:$m_2$ [49:51].

signals at 167, and 162 ppm are due to the methacrylic carbonyl and amide ester carbonyl carbons, respectively. The oxycarbonyl carbon of the both monomeric units is appearing 196 ppm. The group of signals at 115–135 ppm arises from aromatic carbons in the AOEMA and FPAMA units. The signals at 58 and 62 ppm are due to the $OCH_2$ carbons of AOEMA and FPAMA units, respectively. The methyl carbon on the acetyl group signal is observed at 56 ppm.

The IR spectra of the poly(BOEMA-*co*-FPAMA) copolymers show characteristic bands at 1740 $cm^{-1}$ (C=O of ester of the both polymer) and 1760 $cm^{-1}$ (C=O of aryloxycarbonyl), 1680 $cm^{-1}$ (amide ester carbonyl), 3235 $cm^{-1}$ (–NH in the FPAMA unit) 3100–3000 $cm^{-1}$, 1590 $cm^{-1}$ (phenyl), 1160 $cm^{-1}$ (C–O). Peaks at 745–778 $cm^{-1}$ may be assigned to the aromatic C–H out-of-plane bending and 1035–1090 $cm^{-1}$ in-of-plane bending for *p*-disubstitue benzene ring for FPAMA and BOEMA units. The peaks at 700–720 $cm^{-1}$ is due to the aromatic C–H out-of-plane bending of the monosubstitue benzene ring on the benzoyl group.

The $^{1}$H NMR spectrum of poly(BOEMA-*co*-FPAMA) are shown in Fig. 3. The $^{1}$H NMR spectrum of poly(BOEMA-*co*-FPAMA) is consistent with its chemical structure. The signals at 8.5 ppm are due to –NH protons of the FPAMA. The broad peaks at 7.1–7.8 ppm (phenyl protons of monomeric unit), 4.5–5.1 ppm (–$OCH_2$ protons for both monomeric units), 1.7–1.9 ppm (methylene protons of two monomeric units), 0.9–1.1 ppm (other aliphatic protons including those in the backbone). $^{13}$C NMR peak assigments of this copolymer are 48.0 ppm (–$OCH_2$– carbons), 120–146 ppm (aromatic ring carbons), and 167 and 165 ppm (–C=O for methacryl carbonyl and amide ester carbonyl carbons). The oxycarbonyl carbon of the both monomeric units is appearing 183 ppm.

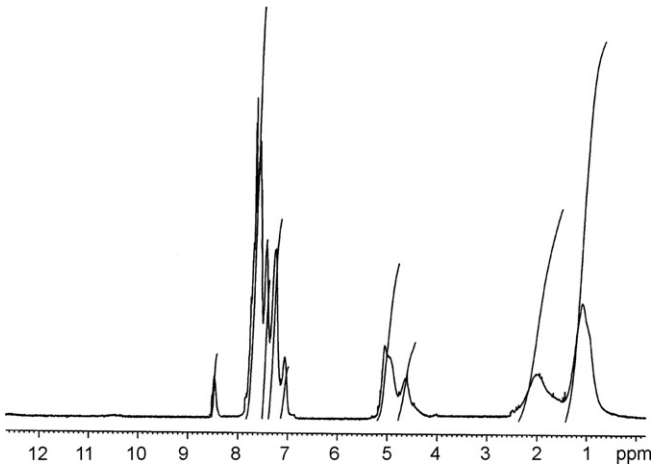


**Fig. 3.** $^{1}$H NMR spectrum of poly(BOEMA-*co*-FPAMA); $m_1$:$m_2$ [45:55].

The main evidence of the polymer formation is certainly the disappearance of some characteristic signals of the double bond in the spectra and this fact was effectively observed in the present study. Thus, two bands vanished in the IR spectrum: the absorption band at 920 $cm^{-1}$ assigned to the C–H bending of geminal $=CH_2$ and the stretching vibration band of C=C at 1633 $cm^{-1}$. From $^{1}$H NMR spectroscopy, the formation of the polymer is also clearly evident from the vanishing of the two singlets at 6.2 and 5.6 ppm of the vinyl protons and the appearance of the broad signal at 2.2–1.7 ppm assigned to an aliphatic $-CH_2-$ group. All the other spectroscopic signals appeared in a normal mode for the macromolecules.

### 2.2. Molecular weights of the polymers

The weight average ($\overline{M}_w$) and number average ($\overline{M}_n$) molecular weights and the polydispersity indexes ($\overline{M}_w/\overline{M}_n$) of polymer samples are presented in Table 1. The number average, weight average molecular weights ($\overline{M}_n, \overline{M}_w$) and the polydispersity index of homopolymers as well as copolymer samples were obtained from gel permeation chromatography. The values of number average and weight average molecular weights of poly(AOEMA-*co*-FPAMA) range from 20,300 to 25,000 and 31,200 to 66,200, respectively. The values of number average and weight average molecular weights of poly(BOEMA-*co*-FPAMA) range from 24,800 to 25,400 and 39,800 to 68,100, respectively. The polydispersity index of homo and copolymers varied in the range of 1.53–2.68 (Table 1). These data clearly indicates that as FPAMA content in the copolymer increases, the molecular weight and polydispersity also increases.

### 2.3. Monomer reactivity ratios

Fineman–Ross (FR), and Kelen–Tudos (KT) methods were used to determine the monomer reactivity ratios. The significance of parameters of FR and KT equations are presented in Table 2.

The graphical plots concerning the methods previously reported are given for poly(AOEMA-*co*-FPAMA) in Fig. 4, whereas the reactivity ratios are summarized in Table 3. In all cases and for all graphical methods the plots were linear indicating that these copolymerizations follow the conventional copolymerization kinetics and that the reactivity of a polymer radical is determined only by the terminal monomer unit.

**Table 1**
Copolymer composition data and molecular weight

| System | $M_2$[a] | $N$[b] (%) | $M_2$[c] | Con. (%) | $M_w \times 10^{-4}$ | $M_n \times 10^{-4}$ | $M_w/M_n$ |
|---|---|---|---|---|---|---|---|
| Poly(AOEMA-*co*-FPAMA) | 0.8 | 4.10 | 0.71 | 7 | 6.02 | 2.38 | 2.52 |
| | 0.7 | 3.54 | 0.62 | 9 | 5.87 | 2.74 | 2.14 |
| | 0.6 | 3.12 | 0.55 | 6 | 5.43 | 2.90 | 1.87 |
| | 0.5 | 2.90 | 0.52 | 8 | 5.16 | 3.01 | 1.71 |
| | 0.4 | 2.85 | 0.51 | 7 | 4.23 | 2.53 | 1.67 |
| | 0.3 | 2.30 | 0.41 | 7 | 3.65 | 2.22 | 1.64 |
| | 0.2 | 1.60 | 0.29 | 9 | 3.12 | 2.03 | 1.53 |
| Poly(BOEMA-*co*-FPAMA) | 0.8 | 3.90 | 0.72 | 7 | 6.81 | 2.54 | 2.68 |
| | 0.7 | 3.35 | 0.65 | 9 | 6.62 | 2.50 | 2.64 |
| | 0.6 | 2.80 | 0.56 | 7 | 6.28 | 2.46 | 2.55 |
| | 0.5 | 2.69 | 0.55 | 8 | 5.57 | 2.38 | 2.34 |
| | 0.4 | 2.45 | 0.51 | 7 | 5.12 | 2.58 | 1.98 |
| | 0.3 | 2.10 | 0.44 | 7 | 4.32 | 2.41 | 1.79 |
| | 0.2 | 1.40 | 0.31 | 8 | 3.98 | 2.48 | 1.60 |

Solvent: 1,4 dioxane, temperature: 65 ± 1 °C, initiator: AIBN (1 wt% of monomers), non-solvent: ethanol.
[a] The mole fraction FPAMA in the feed.
[b] Determined by elemental analyses.
[c] The mole fraction FPAMA in the copolymer.

For both systems the $r_2$ values are higher than the $r_1$ values. The higher $r_2$ value of FPAMA confirms the higher reactivity of FPAMA compared with that of AOEMA or BOEMA. The reactivity ratio values ($r_1$ and $r_2$) of copoly(AOEMA-FPAMA) and copoly(BOEMA-FPAMA) are less than one. Taking into account the microstructures of these copolymer systems, we know that the intermolecular hydrogen bonding between the carbonyl group of AOEMA or BOEMA and the amide group of FPAMA has a larger probability of occurring than the self-association through hydrogen bonding of pure FPAMA [30]. The product $r_1 . r_2$ indicates that the two systems copolymerize randomly in the polymer chain although there is a possible tendency for alternation.

### 2.4. $T_g$'s of the polymers

The $T_g$ values of poly(AOEMA), poly(BOEMA), and poly(FPAMA) obtained under the same conditions with the copolymers were found 92, 98 and 113 °C, respectively. In comparison to that of poly(AOEMA) or poly(BOEMA), the shift to higher temperature is also noted for all the copolymers studied and its magnitude is dependent on the increasing in FPAMA molar fraction in the copolymer chain. An increase in $T_g$ of copolymers may be due to the introduction of comonomer into AOEMA or BOEMA, FPAMA, which increases the intermolecular polar interactions between the molecular chains due to structure stretching. The results clearly indicate that $T_g$ values of copolymers depend on the composition of comonomers and increase with increasing FPAMA contents in the polymer chain. These values are indicated in Table 4. It can be seen that the observed $T_g$ increases with increasing FPAMA and presents a striking positive deviation with respect to linearity, which can be associated with a lower free volume, mobility and flexibility than a mixture of AOEMA or BOEMA and FPAMA units. In addition, the incorporation of polar fluorine atoms in the copolymer backbone resulted in an increase of $T_g$ due to chain stiffening and marked inhibition or rotation about C–C bonds. The presence of strong C–F dipoles in the backbone increases the interaction between the chains.

### 2.5. Thermal analysis

Thermogravimetric curves of the copolymers are compared with those of the homopolymers in Fig. 5. The initial decomposition temperatures of poly(AOEMA) and poly(BOEMA) are around 298 and 260 °C, respectively, and independent of the side-chain structures. This result shows that main-chain scission is an important reaction in the degradation of polymers, at least in the beginning. The degradation of poly(FPAMA) occurred in three stages. The first stage was observed 315–395 °C. The second stage decomposition commenced at 400–425 °C, and the last stage was observed 440–500 °C. The residue at 450 °C for the three polymers is about 10%. The thermal stability of the copolymers was improved by the incorporation of FPAMA. The initial decomposi-

**Table 2**
FR and KT parameters for poly(AOEMA-*co*-FPAMA) and poly(BOEMA-*co*-FPAMA) system

| System | $F = M_1/M_2$ | $f = m_1/m_2$ | $G = F(f-1)/f$ | $H = F^2/f$ | $\mu = G/\alpha + H$ | $\zeta = H/\alpha + H$ |
|---|---|---|---|---|---|---|
| Poly(AOEMA-*co*-FPAMA) | 0.250 | 0.410 | −0.360 | 0.150 | −0.316 | 0.132 |
| | 0.429 | 0.613 | −0.271 | 0.300 | −0.209 | 0.233 |
| | 0.667 | 0.812 | −0.154 | 0.548 | −0.100 | 0.356 |
| | 1.000 | 0.923 | −0.083 | 1.080 | −0.040 | 0.521 |
| | 1.500 | 0.960 | −0.063 | 2.343 | −0.018 | 0.703 |
| | 2.333 | 1.439 | 0.711 | 3.782 | 0.149 | 0.792 |
| | 4.000 | 2.448 | 2.366 | 6.536 | 0.314 | 0.868 |
| Poly(BOEMA-*co*-FPAMA) | 0.250 | 0.389 | −0.393 | 0.161 | −0.317 | 0.130 |
| | 0.429 | 0.538 | −0.368 | 0.342 | −0.260 | 0.241 |
| | 0.667 | 0.786 | −0.182 | 0.566 | −0.111 | 0.345 |
| | 1.000 | 0.812 | −0.083 | 1.080 | −0.040 | 0.521 |
| | 1.500 | 0.960 | −0.063 | 2.343 | −0.018 | 0.703 |
| | 2.333 | 1.272 | 0.498 | 4.279 | 0.092 | 0.799 |
| | 4.000 | 2.226 | 2.203 | 7.188 | 0.267 | 0.870 |

$\alpha$ = 0.990 for the poly(AOEMA-*co*-FPAMA) system and $\alpha$ = 1.076 for the poly(BOEMA-*co*-FPAMA) system.

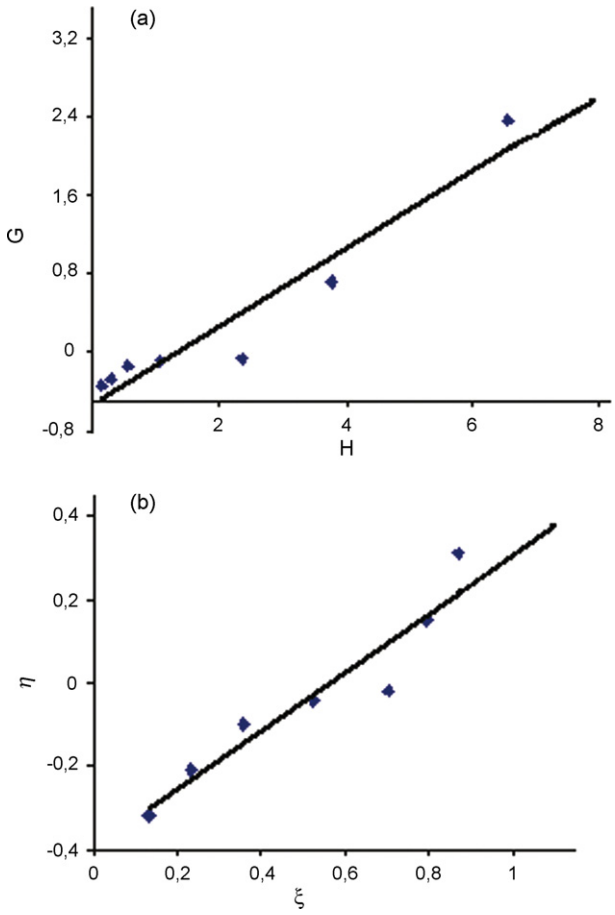


**Fig. 4.** K–T and F–R plot for poly(AOEMA-*co*-FPAMA) system.

**Table 3**
Comparison of reactivity ratios by various methods

| System | Methods | $r_1$ | $r_2$ | $r_1r_2$ | $1/r_1$ | $1/r_2$ |
|---|---|---|---|---|---|---|
| Poly(AOEMA-*co*-FPAMA) | F–R | 0.399 | 0.533 | 0.213 | 2.506 | 1.876 |
| | K–T | 0.310 | 0.393 | 0.122 | 3.226 | 2.545 |
| | Average | 0.355 | 0.463 | 0.164 | 2.817 | 2.160 |
| Poly(BOEMA-*co*-FPAMA) | F–R | 0.350 | 0.554 | 0.194 | 2.857 | 1.805 |
| | K–T | 0.268 | 0.430 | 0.115 | 3.731 | 2.326 |
| | Average | 0.309 | 0.492 | 0.152 | 3.236 | 2.032 |

**Table 4**
The physical parameters and glass transition temperatures of some copolymers

| | $d$ (g cm$^{-3}$) | $\eta_{inh}$ (dl g$^{-1}$) | $\delta$ (cal/cm$^3$)$^{1/2}$ | $T_g$ |
|---|---|---|---|---|
| Poly(AOEMA-*co*-FPAMA) | | | | |
| 29/71 | 1.01 | 0.57 | 10.55 | 110 |
| 45/55 | 1.07 | 0.50 | 11.02 | 105 |
| 59/41 | 1.14 | 0.45 | 11.51 | 96 |
| 71/29 | 1.18 | 0.42 | 11.97 | 94 |
| Poly(BOEMA-*co*-FPAMA) | | | | |
| 28/72 | 1.04 | 0.58 | 9.81 | 111 |
| 44/56 | 1.08 | 0.53 | 10.34 | 108 |
| 56/44 | 1.14 | 0.45 | 11.51 | 102 |
| 69/31 | 1.17 | 0.42 | 11.98 | 100 |
| Poly(FPAMA) | 0.98 | 0.42 | 12.11 | 113 |
| Poly(AOEMA) | 1.21 | 0.60 | 10.43 | 92 |
| Poly(BOEMA) | 1.20 | 0.63 | 10.02 | 98 |

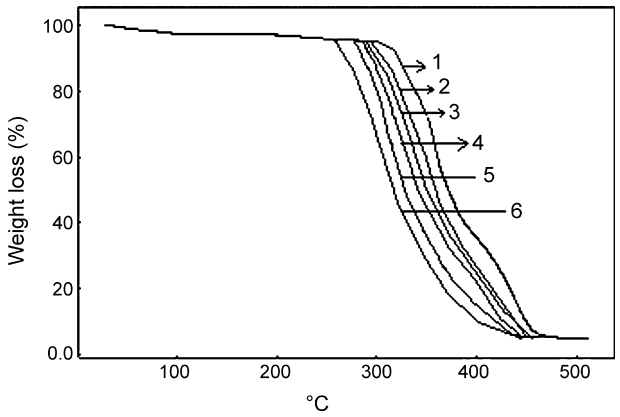


**Fig. 5.** TGA curves for poly(FPAMA) (1), copoly(AOEMA-71% FPAMA) (2), copoly(AOEMA-51% FPAMA) (3), poly(AOEMA) (4), copoly(BOEMA-44% FPAMA) (5) and poly(BOEMA) (6).

tion temperatures of the copolymers were between those of the homopolymers.

### 2.6. Thermal degradation kinetics

In this section, the degradation parameters of polymers are estimated by Ozawa methods. TGA was used to investigate the activation energies. The thermal degradation expression results change according to different assumptions and derivatives, for example, bulk or powder, carrier gas, flow rate, would directly affect the results of parameters [31]. The different analysis methods are described. These methods require several TGA curves at different heating rates. Hence, the dynamic thermogravimetric analysis in nitrogen of the polymers has been performed at various heating rates 7, 10, 15 and 20 °C/min. Fig. 6 shows the TGA curves at the different heating rates of poly(FPAMA).

#### 2.6.1. Ozawa method

According to the method of Ozawa [32], the apparent thermal decomposition activation energy, $E_a$, can be determined from the TGA thermograms under various heating rates with following equation:

$$E_a = -\frac{R}{b}\left[\frac{d\log\beta}{d(1/T)}\right] \quad (1)$$

where $R$ is the gas constant, $b$ is a constant (0.4567), $T$ is the temperature and $\beta$ is the heating rate (°C/min). According to

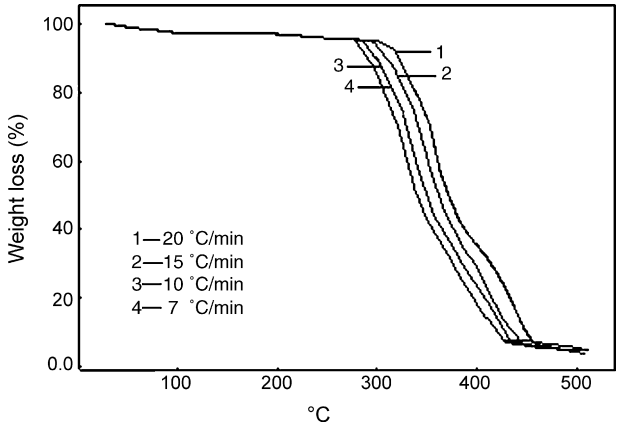


**Fig. 6.** The thermal degradation curves of poly(FPAMA) at different heating rates.

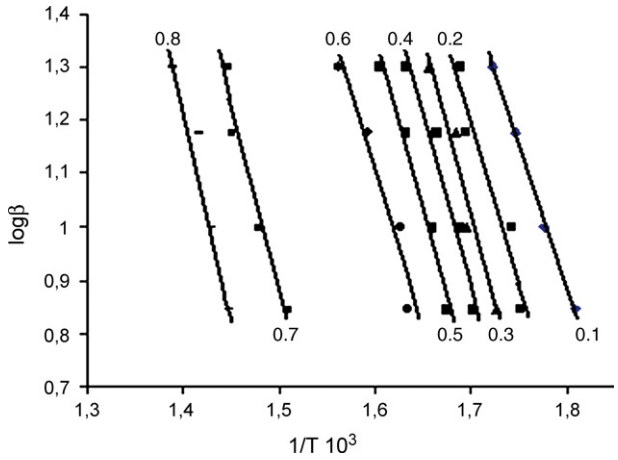


**Fig. 7.** Ozawa's plots of logarithm of heating rate ($\beta$) vs. reciprocal temperature ($1/T$) at different conversions for poly(BOEMA-*co*-FPAMA); $m_1$:$m_2$ [49:51].

Eq. (1), the activation energy of degradation can be determined from the slope of the linear relationship between log $\beta$ and $1/T$. The results of the Ozawa analysis for poly(BOEMA-*co*-FPAMA) are given in Fig. 7, which shows that the best fitting straight lines are nearly parallel, indicating a constant activation energy range of conversions analyzed and confirming the validity of the approach used. Activation energies corresponding to the different conversions are listed in Table 5. $E_a$ calculated from the Ozawa method is superior to other methods for complex degradation, since it does not use the reaction order in the calculation of the decomposition activation energy. Therefore, $E_a$ calculated from the Ozawa method was superior to the former methods for complex degradation.

### 2.7. Antimicrobial effects of the monomers and polymers

The poly(FPAMA) is found to be most effective in inhibiting the growth of microorganisms, and these may be traced to high fluorine content of this homopolymer. Some polymers with side chain amide contents have good biological activity (xx). As expected, compared to poly(FPAMA), poly(AOEMA) or poly(-BOEMA) is less effective to inhibit the growth of microorganisms. Although the fluorine content of the polymers appears to be most important to impart antimicrobial properties, it is possible that the conformation of the polymers acquired under experimental conditions may also be a factor for their antigrowth activity. This study however is beyond the scope of the present investigation. The use of fluorine to increase biological half-life by impeding oxidative metabolism [33], and to increase bioabsorption by lipophilic effects are examples of directed strategies of fluorine substitution. As more data are collected in the literature, it becomes clearer what may be the biological sequelae of a given substitution pattern. In addition, new theories such as polar hydrophobicity [34] help explain increased binding of fluorinated molecules to protein recognition sites. The data are listed in Table 6 and are the average data of three experiments.

## 3. Experimental

### 3.1. Materials

Acetophenone, benzophenone, chloracetylchloride, and sodium hydroxide (Merck), sodium methacrylate, 1,4-dioxane, potassium carbonate, acetonitrile, anhydrous magnesium sulphate (Aldrich) were used as received. 2,2′-Azobisisobutyronitrile was recrystallized from chloroform–methanol. Bactopeptone and glucose was obtained from Difco. All the other chemicals were analytical grade and used without any further purification. AOEMA, BOEMA and FPAMA was prepared as reported [25,26].

### 3.2. Characterization techniques

The FTIR spectrum of molecules was recorded between 4000 and 400 $cm^{-1}$ on a PerkinElmer FTIR System Spectrum BX spectrometer using solid KBr pellet method. The spectrum was recorded at room temperature, with a scanning speed of 10 $cm^{-1}$ $min^{-1}$ and the spectral resolution of 4.0 $cm^{-1}$. $^1H$ and $^{13}C$ NMR spectra were recorded in $CDCl_3$ with tetramethylsilane as the internal standard using on Bruker GmbH DPX-400 400 MHz spectrometer. The glass transition ($T_g$) temperatures were determined by a Shimadzu DSC60H. Samples of about 4–7 mg held in sealed aluminium crucibles and the heating rate of 20 °C/min under a dynamic nitrogen flow (5 l $h^{-1}$) were used for the measurements. From DSC measurements, $T_g$ was taken as the midpoint of the transition region. The thermal stabilities of the polymers were investigated by thermogravimetric analysis in a nitrogen stream at a heating rate of 20 °C $min^{-1}$. The thermal stability of the polymers was determined by Shimadzu TG60H. Molecular weight ($\overline{M}_w$ and $\overline{M}_n$) of the polymers were determined by a water 410 gel permeation chromatography equipped with a differential refractive index detector and calibrated with polystyrene standards. Elemental analyses were carried out by a Elementar CHNSO automicroanalyzer.

### 3.3. Copolymerization

The structure of the monomers is shown in Scheme 2. Copolymerizations of FPAMA with BOEMA and AOEMA using different proportions of FPAMA were carried out in glass ampoules

**Table 5**
The apparent activation energies (kJ/mol) of investigated polymers under thermal degradation in $N_2$

| Sample | 10[a] | 20[a] | 30[a] | 40[a] | 50[a] | 60[a] | 70[a] | 80[a] | 90[a] |
|---|---|---|---|---|---|---|---|---|---|
| Poly(FPAMA) | 158.8 | 163.4 | 166.7 | 160.8 | 164.2 | 166.5 | 163.3 | 160.7 | 162.4 |
| Poly(AOEMA) | 96.73 | 108.39 | 123.36 | 117.32 | 117.25 | 108.11 | 122.28 | 143.85 | 101.73 |
| Poly(BOEMA) | 98.73 | 111.79 | 119.36 | 121.21 | 117.25 | 108.19 | 126.18 | 135.45 | 98.73 |
| Poly(AOEMA-*co*-FPAMA) | | | | | | | | | |
| 29/71 | 182.4 | 171.6 | 181.1 | 186.2 | 185.5 | 185.2 | 182.8 | 185.0 | 187.1 |
| 48/52 | 169.6 | 175.0 | 168.2 | 171.4 | 169.9 | 173.8 | 177.7 | 169.6 | 182.4 |
| 71/29 | 155.5 | 158.2 | 171.8 | 173.2 | 170.6 | 168.0 | 173.1 | 168.2 | 176.8 |
| Poly(BOEMA-*co*-FPAMA) | | | | | | | | | |
| 28/72 | 224.9 | 229.2 | 232.8 | 233.1 | 234.8 | 231.4 | 229.8 | 232.8 | 230.5 |
| 45/55 | 216.4 | 215.1 | 216.3 | 217.6 | 222.6 | 219.9 | 222.0 | 221.9 | 218.9 |
| 69/31 | 211.6 | 209.7 | 211.7 | 208.5 | 213.2 | 207.9 | 214.7 | 217.5 | 213.2 |

[a] Conversion (%).

**Table 6**
Antimicrobial effects of the compounds (mm of zones)

| Compounds | *Pseudomonas aeruginasa* | *Escherichia coli* | *Proteus vulgaris* | *Salmonella enteridis* | *Klebsiella pneumoniae* | *Staphylococcus aureus* | *Candida albicans* |
|---|---|---|---|---|---|---|---|
| Poly(FPAMA) | 17 | 16 | 14 | 15 | 15 | 17 | 16 |
| Poly(AOEMA) | 13 | 12 | – | – | – | 14 | – |
| Poly(BOEMA) | 14 | 13 | 12 | 10 | – | 13 | – |
| Poly(AOEMA-*co*-FPAMA) | | | | | | | |
| 29/71 | 18 | 17 | 13 | – | 17 | 12 | – |
| 48/52 | 16 | 16 | | 16 | – | 10 | – |
| 71/29 | 15 | 14 | 12 | – | 13 | 9 | 15 |
| Poly(BOEMA-*co*-FPAMA) | | | | | | | |
| 28/72 | 18 | 18 | 17 | 16 | 14 | 18 | 14 |
| 45/55 | 16 | 17 | 15 | – | 13 | 16 | – |
| 69/31 | 15 | 14 | 13 | 12 | – | 15 | – |
| Penicillin G | 18 | 15 | 9 | 19 | 21 | 19 | 35 |
| Teicoplanin | 19 | 19 | 21 | 23 | 27 | 14 | 19 |
| DMSO | – | – | – | – | – | – | – |

Compound concentration: 100 μg/disc; the symbol (–) reveals that the compounds have no activity against the microorganisms. DMSO: Dimethylsulfoxide (control).

under $N_2$ atmosphere in 1,4-dioxane solution with AIBN (1%, based on the total weight of monomers) as an initiator. The reacting components were degassed by threefold freeze–thawing cycle and then immersed in a oil bath at 65 ± 0.1 °C for a given reaction time. The reaction time was selected to give conversions less than 10% to satisfy the differential copolymerization equation. After the desired time the copolymers were separated by precipitation in ethanol and reprecipitated from $CH_2Cl_2$ solution. The copolymers, purified by reprecipitation to avoid the formation of homopolymers. The copolymers were finally dried over vacuum at 45 °C to constant weight. The amounts of monomeric units in the copolymers were determined by elemental analysis. The results are presented in Table 1.

### 3.4. Determination of the monomer reactivity ratios

The monomer reactivity ratios for the copolymerization of AOEMA and BOEMA with FPAMA were determined from the monomer feed ratios and the copolymer composition. The Fineman–Ross (FR), and Kelen–Tudos (KT) methods were used to determine the monomer reactivity ratios.

According to the FR method, the monomer reactivity ratios can be obtained as follows:

$$G = Hr_1 - r_2 \tag{1}$$

where $r_1$ and $r_2$ correspond to the AOEMA or BOEMA and FPAMA monomers, respectively. The parameters $G$ and $H$ are defined as follows:

$$G = \frac{F}{(f-1)/f} \quad \text{and} \quad H = \frac{F^2}{f} \tag{2}$$

with

$$F = \frac{M_1}{M_2} \quad \text{and} \quad f = \frac{m_1}{m_2} \tag{3}$$

where $M_1$ and $M_2$ are the monomer molar compositions in the feed and $m_1$ and $m_2$ are the copolymer molar compositions.

Alternatively, the reactivity ratios can be obtained with the KT method, which is based on the following equation:

$$\eta = \left(r_1 + \frac{r_2}{\alpha}\right)\xi - \frac{r_2}{\alpha} \tag{4}$$

where $\eta$ and $\xi$ are the functions of the parameters $G$ and $H$

$$\eta = \frac{G}{\alpha + H} \quad \text{and} \quad \xi = \frac{H}{\alpha + H}, \tag{5}$$

and $\alpha$ is a constant equal to $(H_{max}H_{min})^{1/2}$, $H_{max}$ and $H_{min}$ being the maximum and minimum $H$ values, respectively, from the series of measurements. From a linear plot of $\eta$ as a function of $\xi$, the values of $\eta$ for $\xi = 0$ and $\xi = 1$ can be used to calculate the reactivity ratios according to the following equations:

$$\xi = 0 \rightarrow \eta = \frac{-r_2}{\alpha} \quad \text{and} \quad \xi = 1 \rightarrow \eta = r_1 \tag{6}$$

### 3.5. Determination of the physical parameters of the polymers

Some physical parameters such as density ($d$), solubility parameter ($\delta$) and inherent viscosity ($\eta_{inh}$) of the polymers were determined in this study. The densities of the polymers were determined experimentally by the flotation method [29] at 25 °C using mixtures of methanol and formic acid as the floating agent, and

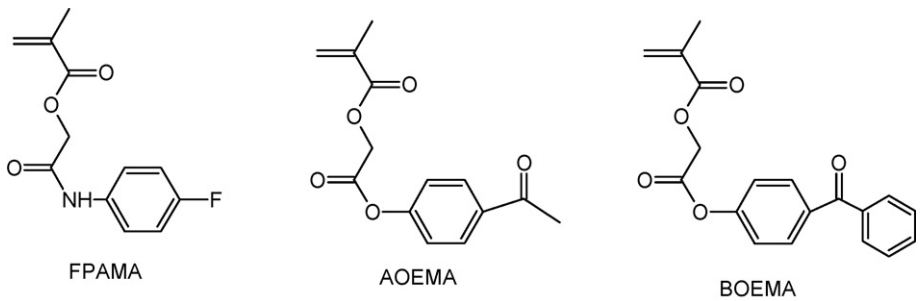


**Scheme 2.**

many glass beads of known densities. The solubility parameters of the polymers were determined by using a titration method [29] at 25 °C from a solubility test using $CH_2Cl_2$ as a solvent and *n*-hexane and ethanol as non-solvent. Solutions of the polymers in $CHCl_3$ at the concentration of 0.5 g $dl^{-1}$ were used to determine inherent viscosities ($\eta_{inh} = \ln \eta_r/C$). Measurements were performed by an Ubbelohde viscometer thermostatted at 25 °C. These values of the physical parameters of copolymers depend on the composition of comonomers. The results are shown in Table 3.

### 3.6. Biological activity of the polymers

The biological activities of the homopolymers and copolymers were tested against different microorganisms with DMSO as the solvent. The sample concentrations were 100 μg/discH. All microorganism strains were obtained from the Culture Collection of Microbiology Laboratory of Afyon Kocatepe University (Afyon, Turkey). In this study, *Staphylococcus aureus* ATCC 29213, *Escherichia coli* ATCC 25922, *Pseudomonas aeruginasa* ATCC 27853, *Proteus vulgaris*, *Salmonella enteridis*, and *Klebsiella pneumoniae* were used as bacteria. *Candida albicans* CCM 31 was a fungus. YEPD medium cell culture was prepared as described by Connerton [35]. Ten milliliters of YEPD medium were inoculated with each cell from plate cultures. Yeast extract 1% (w/v), bactopeptone 2% (w/v), and glucose 2% (w/v), was obtained from difco. Microorganisms were incubated at 35 °C for 24 h. About 1.5 ml of these overnight stationary phase cultures were inoculated onto 250 ml of YEPD and incubated at 35 °C until $OD_{600}$ reached 0.5. The antibiotic sensitivity of the polymers was tested with the antibiotic disk assay as described [36]. Nutrient Agar (NA) was purchased from Merck. About 1.5 ml of each prepared different cell culture were transferred into 20 ml of NA and mixed gently. The mixture was inoculated into the plate. The plates were rotated firmly and allowed to dry at room temperature for 10 min. Prepared antibiotic discs (100 μg/disc) were placed on the surface of the agar medium [37]. The plates were kept at 5 °C for 30 min and then incubated at 35 °C for 2 days. If a toxic compound leached out from the disc, it means that the microbial growth is inhibited around the sample. The width of this area expressed the antibacterial or antifungal activity by diffusion. The zones of inhibition of microorganism growth of the standard samples polymers were measured with a millimeter ruler at the end of the incubation period.

## 4. Conclusion

Copolymers of AOEMA and BOEMA with FPAMA have been prepared by free-radical polymerization in 1,4-dioxane at 65 °C. The reactivity ratios of the copolymers were estimated using linear graphical methods. The $r_2$ values were higher than the corresponding $r_1$ values in all cases, meaning that a kinetic preference exists for the incorporation of FPAMA in the copolymer structure. The glass transition temperatures of the AOEMA and BOEMA with FPAMA copolymers were obtained and compared. The TGA studies concluded that the thermal stability of the copolymers increases with an increase of FPAMA in the copolymer chain. The biological activity and thermal stability of the polymers were investigated. The biological activity of the polymers increases with an increase in the mole fraction of FPAMA in the copolymers. The decomposition activation energies of the polymers were calculated with the Ozawa method.

## Acknowledgement

The authors are indebted to Dr. Elif Korcan for the biological activity studies.

## References

[1] L. van Ravenstein, W. Ming, R.D. van de Grampel, R. van der Linde, G. de With, T. Loontjens, P.C. Thune, J.W. Niemantsverdriet, Macromolecules 37 (2) (2004) 408–413.
[2] H.M. Wei, V.R. Luc, V.D.G. Robert, Polym. Bull. 47 (2001) 321–328.
[3] I.J. Park, S.B. Lee, C.K. Choi, Polymer 38 (1997) 2523–2527.
[4] B. Ameduri, R. Bongiovanni, G. Malucelli, A. Pollicino, A. Priola, J. Polym. Sci., Part A: Polym. Chem. 37 (1999) 77–87.
[5] V. Pomes, A. Fernandez, N. Costarramone, B. Grano, D. Houi, Colloid Surf. A 2–3 (1999) 481–490.
[6] S. Yang, J. Wang, K. Ogino, S. Valiyaveettil, C.K. Ober, Chem. Mater. 12 (2000) 33–40.
[7] J.R. Lee, F.L. Jin, S.J. Park, J.M. Park, Surf. Coat. Technol. 180–181 (2004) 650–654.
[8] E. Sacher, Prog. Surf. Sci. 47 (1994) 273–300.
[9] F.R. Pu, R.L. Williams, T.K. Markkula, J.A. Hunt, Biomaterials 23 (2002) 2411–2428.
[10] H. Tanaka, T. Takeichi, T. Hongo, J. Polym, Sci. Part A: Polym. Chem. 35 (1997) 3537–3541.
[11] I.J. Park, S.B. Lee, C.K. Choi, Macromolecules 31 (1998) 7555–7558.
[12] K. Li, P.P. Wu, Z.W. Han, Polymer 43 (2002) 4079–4086.
[13] T. Nishino, Y. Urushihara, M. Meguro, K. Nakamae, J. Colloid Interface Sci. 279 (2004) 364–369.
[14] S.M. Walz, T.E. Malner, U. Mueller, R. Muelhaupt, J. Polym. Sci., Part B: Polym. Phys. 41 (2003) 360–367.
[15] R.F. Linemann, T.E. Malner, R. Brandsch, G. Bar, W. Ritter, R. Mulhaupt, Macromolecules 32 (6) (1999) 1715–1721.
[16] R.R. Thomas, K.G. Lloyd, L.M. Stika, L.E. Stephans, G.S. Magallanes, V.L. Dimonie, E.D. Sudol, M.S. El-Aasser, Macromolecules 33 (2000) 8828–8841.
[17] K. Landfester, R. Rothe, M. Antonietti, Macromolecules 35 (2002) 1658–1662.
[18] S.Y. Cheng, Y.J. Chen, Z.G. Chen, J. Appl. Polym. Sci. 85 (2002) 1147–1153.
[19] J.W. Ha, I.J. Park, S.B. Lee, D.K. Kim, Macromolecules 35 (2002) 6811–6818.
[20] P. Marion, G. Beinert, D. Juhúe, J. Lang, Macromolecules 30 (1997) 123–129.
[21] P. Marion, G. Beinert, D. Juhúe, J. Lang, J. Appl. Polym. Sci. 64 (1997) 2409–2419.
[22] C.C. Zhang, Y.J. Chen, Polym. Int. 54 (2005) 1027–1033.
[23] T.C. Chang, W.Y. Shen, Y.S. Chiu, H.B. Chen, S.Y. Ho, J. Polym. Sci. Part A: Polym. Chem. 34 (1996) 3337–3343.
[24] T.C. Chang, H.B. Chen, Y.S. Chiu, S.Y. Ho, Polym. Degrad. Stab. 57 (1997) 7–14.
[25] I. Erol, C. Soykan, React. Funct. Polym. 56 (2003) 147–157.
[26] I. Erol, C. Soykan, J. Macromol. Sci. Pure Appl. Chem. A39 (2002) 405–417.
[27] M. Fineman, S.D. Ross, J. Polym. Sci. 5 (1950) 259.
[28] T. Kelen, F. Tudos, J. Macromol. Sci. Chem. 9 (1975) 1.
[29] E.C.Z. Chan, M.J. Pelczar, N.R. Krieg, Agar Diffusion Method, in: Chan, et al. (Eds.), Laboratory Exercies in Microbiology, McGraw-Hill, New York, 1993, p. 225.
[30] W.K. Shiao, C.K. Hsin, C.C. Feng, Polymer 44 (2003) 6873–6882.
[31] H.H.G. Jellinek, M.D. Luh, J. Phys. Chem. 70 (1966) 3672–3680.
[32] T. Ozawa, Bull. Chem. Soc. Jpn. 38 (1965) 1881–1886.
[33] P.N. Edwards, in: R.E. Banks, B.E. Smart, J.C. Tatlow (Eds.), Organo Fluorine Chemistry, Principles and Commercial Applications, Plenum Press, New York, 1994, pp. 501–541.
[34] D. Kim, L. Wang, M. Beconi, G.J. Eiermann, M.H. Fisher, H. He, G.J. Hickey, J.E. Kowalchick, B. Leiting, K. Lyons, F. Marsilio, M.E. McCann, R.A. Patel, A. Petrov, G. Scapin, S.B. Patel, R.S. Roy, J.K. Wu, M.J. Wyvratt, B.B. Zhang, L. Zhu, N.A. Thornberry, A.E. Weber, J. Med. Chem. 48 (2005) 141–151.
[35] I.F. Connerton, in: G.W. Gould (Ed.), Analysis of Membrane Proteins, Portland, London, 1994, p. 177.
[36] E.L. McCafferty, Laboratory Preparation for Macromolecular Chemistry, McGraw-Hill, New York, 1970, p. 22.
[37] J.A. Desai, U. Dayal, P.H. Parsania, J. Macromol. Sci. Pure Appl. Chem. 33 (1996) 1113–1122.